Cell, Vol. 121, 437–450, May 6, 2005, Copyright ©2005 by Elsevier Inc. DOI 10.1016/j.cell.2005.02.017

Modulation of Receptor Recycling and Degradation by the Endosomal Kinesin KIF16B

Sebastian Hoepfner,[1] Fedor Severin,[1,4] Alicia Cabezas,[2,4] Bianca Habermann,[1] Anja Runge,[3] David Gillooly,[2] Harald Stenmark,[2] and Marino Zerial[1,*]

[1]Max-Planck Institute for Molecular Cell Biology and Genetics
Pfotenhauerstrasse 108
D-01307 Dresden
Germany

[2]The Norwegian Radium Hospital
Department of Biochemistry
Montebello, N-0310 Oslo
Norway

[3]HHMI/University of Pennsylvania University Cancer Center
421 Curie Boulevard
Philadelphia, Pennsylvania 19104

Summary

Different classes of endosomes exhibit a characteristic intracellular steady-state distribution governed by interactions with the cytoskeleton. We found a kinesin-3, KIF16B, that transports early endosomes to the plus end of microtubules in a process regulated by the small GTPase Rab5 and its effector, the phosphatidylinositol-3-OH kinase hVPS34. In vivo, KIF16B overexpression relocated early endosomes to the cell periphery and inhibited transport to the degradative pathway. Conversely, expression of dominant-negative mutants or ablation of KIF16B by RNAi caused the clustering of early endosomes to the perinuclear region, delayed receptor recycling to the plasma membrane, and accelerated degradation. These results suggest that KIF16B, by regulating the plus end motility of early endosomes, modulates the intracellular localization of early endosomes and the balance between receptor recycling and degradation. We propose that this mechanism could have important implications for signaling.

Introduction

The endocytic system is composed of a series of biochemically and morphologically distinct organelles that carry out specialized tasks in the uptake, recycling, and catabolism of growth factors and nutrients, serving a plethora of key biological functions (Mellman, 1996). These functions require the interaction of endocytic organelles with the actin and tubulin cytoskeleton. Actin- and microtubule-dependent motors generate the forces required to drive vesicle formation and delivery to their target compartment (Howard et al., 1989). For example, the unconventional myosin VI motor propels clathrin-coated vesicles through the cortical actin mesh underneath the plasma membrane toward early endosomes (Aschenbrenner et al., 2004). Motor proteins also serve several other important tasks, such as cargo sorting through membrane tubulation and fission, endosome inheritance, and positioning (Goldstein, 2001; Goodson et al., 1997; Hirokawa et al., 1998). Endosomes have a characteristic intracellular distribution and exhibit both short- and long-range movements with a wide range of velocities (Gasman et al., 2003; Nielsen et al., 1999; Valetti et al., 1999). Whereas early endosomes are dispersed throughout the cytoplasm, recycling endosomes, late endosomes, and lysosomes are typically situated in close proximity to the nucleus. This distribution pattern observed at steady state results from a dynamic interaction of endosomes with the cytoskeleton. The minus end motor dynein-dynactin complex is responsible for the perinuclear localization of endosomes and lysosomes (Allan, 2000; Burkhardt et al., 1997) but also for early-to-late endosome transport (Aniento et al., 1993). Plus end, kinesin-dependent motility facilitates exocytosis of cargo from recycling endosomes to the cell surface (Lin et al., 2002). Microtubule-dependent motility supports endocytic trafficking between apical early and recycling endosomes as well as transcytosis in polarized epithelial cells (Apodaca, 2001). However, a requirement for microtubule-dependent transport has been demonstrated neither for endocytosis nor for recycling from early endosomes to the plasma membrane, which depends, rather, on actin (Apodaca, 2001). Furthermore, it remains unclear which microtubule motors besides dynein control the intracellular distribution and motility of early endosomes and how their function is integrated with the sorting and transport of cargo.

Increasing evidence points at a role of Rab-GTPases in coordinating membrane tethering and fusion with cytoskeleton-dependent organelle motility (Echard et al., 1998; Jordens et al., 2001; Zerial and McBride, 2001). On early endosomes, the small GTPase Rab5 coordinates the activity of several effector proteins that cooperatively regulate endocytic trafficking (Zerial and McBride, 2001). A key effector of Rab5 is the phosphatidylinositol-3-OH kinase (PI3-K) hVPS34/p150 that, by generating PI(3)P in proximity to Rab5, allows the recruitment of Rab5 effectors bearing the PI(3)P binding FYVE motif. The concerted activity of Rab5 and hVPS34 is also required for bidirectional, microtubule-based, endosome motility in vitro (Nielsen et al., 1999), raising the question of which molecular motor(s) may function downstream.

The superfamily of kinesin proteins (KIF) drives a great variety of microtubule-dependent motility events (Goldstein, 2001; Goodson et al., 1997; Hirokawa et al., 1998). Each kinesin contains a conserved "motor domain" as well as a variable tail, mediating cargo specificity. The Unc104/KIF1A kinesin, which transports synaptic vesicle precursors, utilizes its pleckstrin homology (PH) "tail domain" to bind directly to PI(4,5)P_2 lipids (Klopfenstein et al., 2002).

The finding that Rab5-dependent early endosome

*Correspondence: zerial@mpi-cbg.de
[4]These authors contributed equally to this work.

A

B

```
                  α6>   <β9> <β10> <   α7
HsKif16B     353  NRAKNIINKPTINEDA----NVKLIRELRAEIARLKTLLA----------QGNQIALLDSPT  400
HsKif1A      349  DRAKQIRCNAVINEDP----NNKLIRELKDEVTRLRDLLYA---------QGLGDITDMTNA  397
HsKHC        320  QRAKTIKNTVCVNVELTAEQWKKKYEKEKEKNKILRNTIQWLENELNRWRNGETVPIDEQFD  381
                    * *      **     abcdefgabcdefgabcdefgabcdefgabcd
```

C

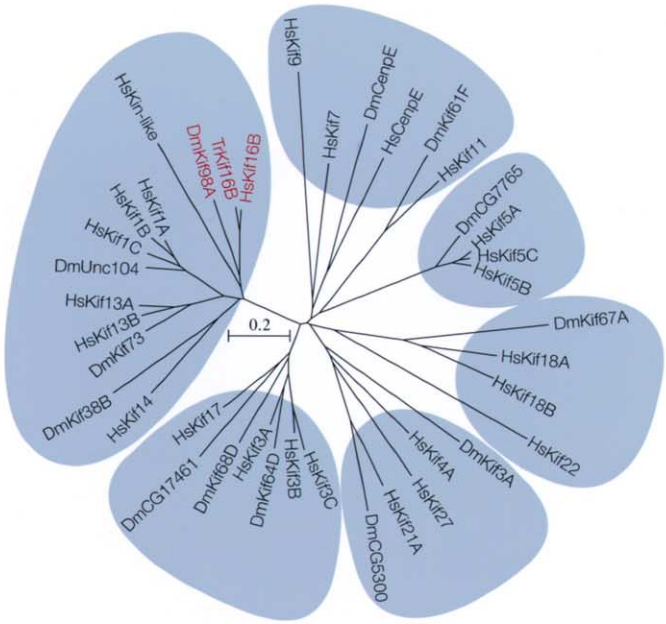

D

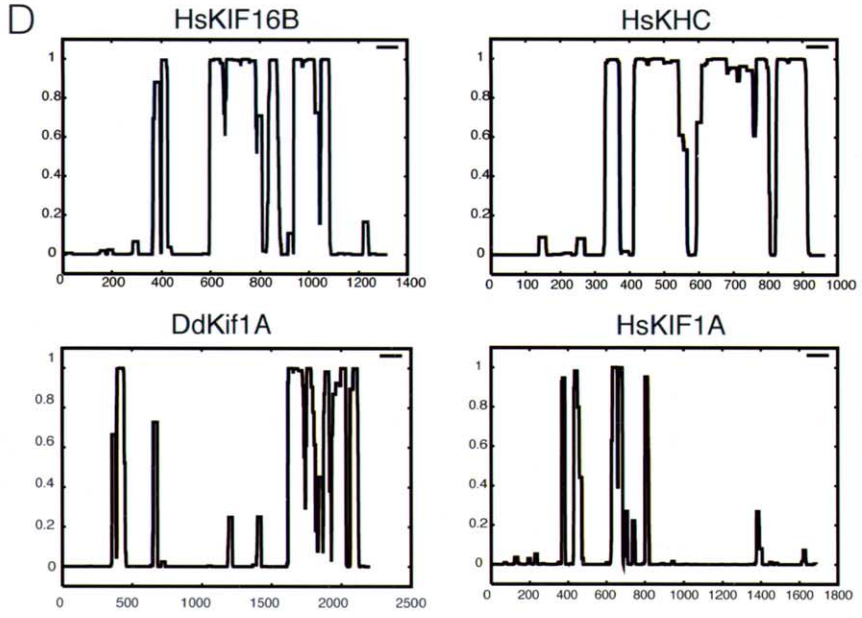

motility depends on PI(3)P raises the possibility that this lipid may recruit an adaptor of a motor or, in the simplest case, a motor itself (Nielsen et al., 1999). To date, two distinct conserved structural motifs, the FYVE finger and the PhoX homology (PX) domain, are known to bind PI(3)P (Lemmon, 2003). Here, we searched for motor proteins displaying such motifs.

Results

Identification and Cloning of the Kinesin KIF16B

A genome sequence database search was devised to identify candidate kinesins harboring either a FYVE or PX motif. This search revealed a gene encoding a putative motor protein with a C-terminal PX domain in *D. melanogaster* (DmKLP98A) as well as a previously unknown ortholog in Fugu *T. rubripes* (JGI32205). The paucity of introns in the Fugu genome, together with the high similarity of the Fugu kinesin to the human ortholog, enabled us to predict the equivalent open reading frame in *H. sapiens* (KIF16B, accession number BX647572). To our knowledge, next to KIF1A, KIF16B represents the only other example of an evolutionary conserved kinesin-like protein, bearing a putative lipid binding domain across all genomes sequenced so far. A cDNA encoding full-length hsKIF16B was cloned and found, in comparison to the BX647572 cDNA, to contain a single nucleotide polymorphism (SNP) at position 820 (G820A). KIF16B is a protein of 1318 amino acid residues with a deduced molecular weight of 152 kDa (Figure 1A). It is predicted to be a plus end motor protein on the basis of (1) the N-terminal localization of the structurally conserved catalytic domain (amino acids 1–355) and (2) the presence of four conserved amino acids C-terminally to the α-6 helix (Figure 1B) (Case et al., 1997).

According to the recent nomenclature (Lawrence et al., 2004), KIF16B is a member of the kinesin-3 family, encompassing a total of eight members in the human genome (Figure 1C). Its closest paralogue in *H. sapiens* is KIF1A, sharing 59% sequence identity in the motor domain. KIF16B displays two diagnostic properties of the kinesin-3 family, a conserved insertion in loop 3 and a forkhead homology (FHA) domain in its stalk (Vale, 2003). Kinesins of this family are thought to exist either as monomers like hsKIF1A (accession number CAA62346) or dimers such as DdKIF1A (accession number X65873), depending on the presence of coiled-coil motifs (Vale, 2003). Using the COILS algorithm (Lupas et al., 1991), we compared the predicted content in coiled-coil structure of KIF16B with all human kinesin-3 family members and deduced that KIF16B has a much higher coiled-coil propensity in its stalk, analogous to that of dimeric *D. discoideum* KIF1A and KHC (Pollock et al., 1999) (Figure 1D).

Whereas many KIFs are primarily expressed in brain (Miki et al., 2003), KIF16B is also present in various other organs, e.g., kidney, liver, intestine, placenta, leukocytes, heart, and skeletal muscle by Northern and Western blot analysis (see Figure S1 in the Supplemental Data available with this article online), in agreement with the broad expression pattern for this gene (C20orf23) reported in the genome-wide expression database GeneNote (Shmueli et al., 2003).

KIF16B Is a Plus End-Directed Motor

Recombinant KIF16B expressed and purified from a baculovirus system was tested for the directionality of movement using an in vitro assay based on polarity-marked microtubules (Hyman, 1991). In this assay, taxol-stabilized microtubules with bright fluorescent plus ends move on a glass slide coated with the motor protein. In line with our bioinformatics prediction, the majority of microtubules (24 out of 28) were found to glide toward their dimly labeled minus ends (Figure 2A). Purified KIF16B mediated microtubule gliding with velocities between 0.175 and 0.275 μm/s (Figure 2B). These values are in the same range of long-distance movements of early endosomes in vivo, typically displaying velocities of ~0.3μm/s (Gasman et al., 2003) (Supplemental Data). The velocity depends both on the intrinsic properties of the catalytic domain and the stability of the coiled coil in the neck (Vale, 2003). Although the neck of KIF16B is similar to that of KIF1A (Figure 1C), it differs considerably in the coiled-coil propensity of its stalk (Figure 1) and in its velocity (~1.20 μm/s in vitro [Okada et al., 1995] and 1.02 μm/s in vivo [Zhou et al., 2001] for KIF1A).

KIF16B Is Localized to PI(3)P-Containing Early Endosomes In Vivo

A key feature of KIF16B is the PX domain at the C terminus that could target the motor to early endosomes via binding to PI(3)P. We measured the binding kinetics of the PX domain of KIF16B fused to GST (GST-CtermPX) by plasmon resonance using a sensor chip coated with different PIs (Figure 2C). Whereas the PX domain of KIF16B did not bind to PI(4,5)P2, unlike KIF1A and Unc104 motors (Klopfenstein et al., 2002), it bound to PI(3)P, PI(3,4)P2, and PI(3,4,5)P3 with affinities (K_D = 28

Figure 1. KIF16B, a Close Paralog to KIF1A, Exhibits Structural Properties of a Dimeric, Plus End-Directed Kinesin

(A) Conserved domains within HsKIF16B include the N-terminal kinesin motor domain (KISc), the forkhead domain (FHA), and the PX domain at the C terminus.

(B) The kinesin KIF16B is most closely related to HsKIF1A.

(C) The putative neck linker region (blue), the neck (yellow), and part of the hinge region (green) of HsKIF16B were aligned against HsKIF1A as well as HsKHC. The heptad repeats are very similar to KIF1A. Asterisks (*) mark residues that are well conserved in plus ended-directed motors, and predicted β sheets as well as α helices are indicated above the alignment.

(D) COILS prediction of coiled-coil structures within HsKIF1A and KIF16B as well as KHC. Scores above 0.5 represent significant probability that coiled-coil structures are present.

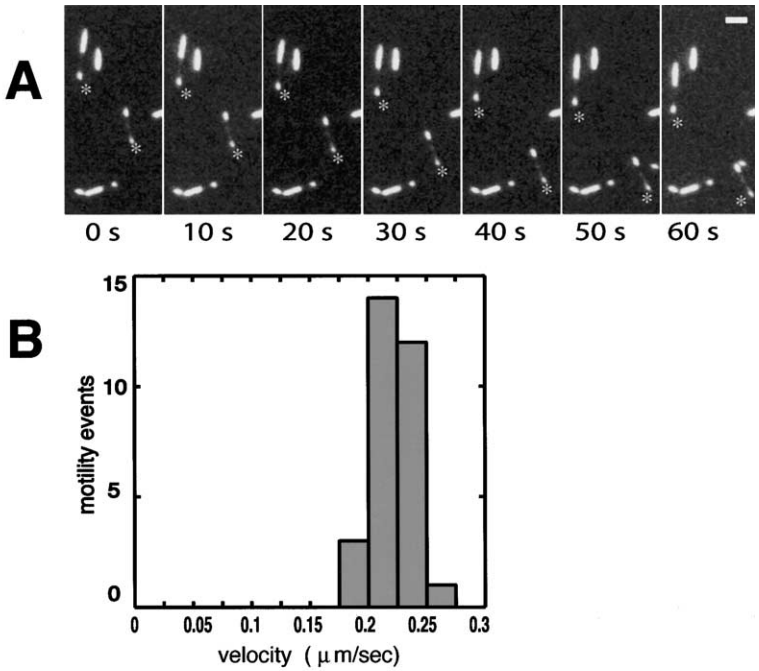

C

Binding affinities of PX to different phosphoinositides

Phosphoinositide	K_D(nM) GST-CtermPX	K_D(nM) GST-Cterm ΔPX
PI(3)P	28 +/- 11*	NDB***
$PI(3,4)P_2$	40 +/- 24**	
$PI(3,4,5)P_3$	99 +/- 55**	
$PI(4,5)P_2$	NDB***	

* from 5 experiments
** from 2 experiments
*** NDB not detectable binding

Figure 2. KIF16B Is a Processive, Plus End-Directed Motor and Binds PI(3)P through its PX Motif

(A) Video microscopy was used to capture movements of labeled microtubules over a lawn of kinesin molecules on a glass slide. Each microtubule carries a short stretch of fluorescently labeled tubulin on its minus end. The still images shown reveal movement of microtubules in direction of their minus ends (*), driven by the plus end motility of the kinesins.

(B) Velocity distribution of the microtubules in (A). Each recorded motility event represents microtubules continuously moving for at least three consecutive frames without switching direction.

(C) GST-KIF16B-PX protein was injected into plasmon resonance sensor chips loaded with liposomes containing 2 mol% of each PI. An average K_D was obtained for each PI. No binding (signal below baseline level, i.e., less than 2 RU) was observable for GST protein alone and GST-KIF16B-PX and PI(3,4)P2.

nM, 40 nM, and 99 nM, respectively) comparable to those reported for the FYVE domain of Hrs binding to PI(3)P (K_D of 38 ± 19 nM) (Gillooly et al., 2000).

Whereas FYVE fingers specifically interact with PI(3)P, PX domains generally do not exhibit the same selectivity (Lemmon, 2003). Since PI(3)P is localized to endosomes, while both PI(3,4)P2 and PI(3,4,5)P3 are typically found at the plasma membrane, we next determined the intracellular localization of KIF16B in vivo. An affinity-purified rabbit antiserum raised against recombinant, truncated (headless) KIF16B protein (see Experimental Procedures) detected the endogenous protein by confocal immunofluorescence microscopy and Western blot analysis (see below). In HeLa cells (Figure 3A), endogenous KIF16B almost completely overlapped with myc-tagged double FYVE serving as a probe for PI(3)P on early endosomes (Gillooly et al., 2000). Given the background nuclear staining of the antibody (persisting by labeling with the preimmune serum or upon ablation of KIF16B by RNAi, see Figure 6G), we verified that exogenous KIF16B also localized to PI(3)P-positive early endosomes (Figure 3B). No evidence for plasma membrane localization could be obtained. Importantly, at low expression levels, the exogenous KIF16B motor did not significantly alter the distribution of early endosomes (see below).

In view of the binding of the KIF16B PX motif to PI(3)P in vitro, we next tested whether this phospholipid is required for targeting KIF16B fused to YFP (KIF16B-YFP) to early endosomes (Gillooly et al., 2000). The generation of PI(3)P can be inhibited pharmacologically, with the fungal toxin Wortmannin or LY294002 (see below). Upon treatment with 100 nM Wortmannin, most KIF16B-YFP detached from endosomes, leading to a diffuse cytosolic staining pattern (Figures 3C and 3D). EEA1, which localizes to the Rab5 domain of early endosomes PI(3)P dependently (Zerial and McBride, 2001), served as a positive control.

On early endosomes, Rab5 recruits effectors bearing the FYVE domain via a dual mechanisms, i.e., (1) by direct binding and (2) through generation of PI(3)P via interaction with the PI3-K hVPS34/p150 (Zerial and McBride, 2001). While we were unable to detect specific binding of KIF16B to Rab5 in vitro (data not shown), expression of dominant-negative Rab5S34N caused the release of KIF16B from endosomes in vivo (Figures 3E and 3F). This suggests that the membrane localization of KIF16B most likely depends on Rab5-mediated PI(3)P production. Altogether, the above experiments provide strong evidence that KIF16B is localized to PI(3)P-positive early endosomes in a Rab5- and PI3-K-dependent manner in vivo.

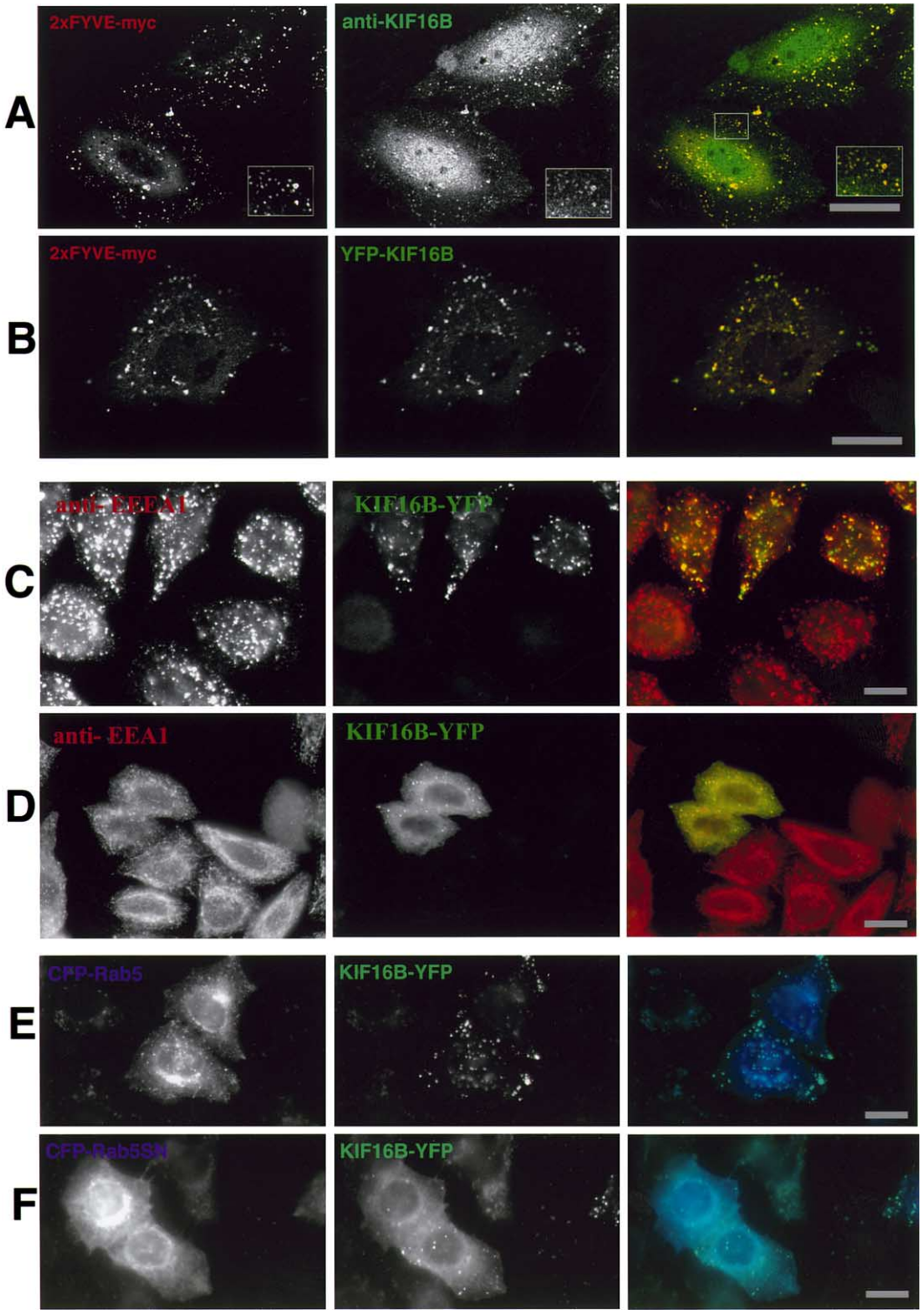

Figure 3. The Kinesin KIF16B Requires the Presence of PI(3)P as well as Rab5 Activity to Localize to Endosomes

HeLa cells were transfected with the PI(3)P lipid probe 2xFYVE-myc as well as with KIF16B-YFP prior to immunofluorescence microscopy with anti-myc and anti-Kif16B antisera. The confocal images show almost complete colocalization of endogenous (A) and ectopic (B) KIF16B with the endosomal marker 2xFYVE. (C) To examine the interaction of KIF16B and PI(3)P in vivo, transfected cells expressing KIF16B-YFP were incubated in the presence (D) or absence (C) of 100 nM Wortmannin for 20 min at 37°C and then processed for immunofluorescence for EEA1. (E) HeLa cells were cotransfected with KIF16B-YFP (green) and Rab5-CFP (blue) or KIF16B-YFP and dominant-negative Rab5-S34N-CFP (F). Overexpression of the Rab5 mutant results in release of KIF16B to the cytosol. Scale bars, 20 μm.

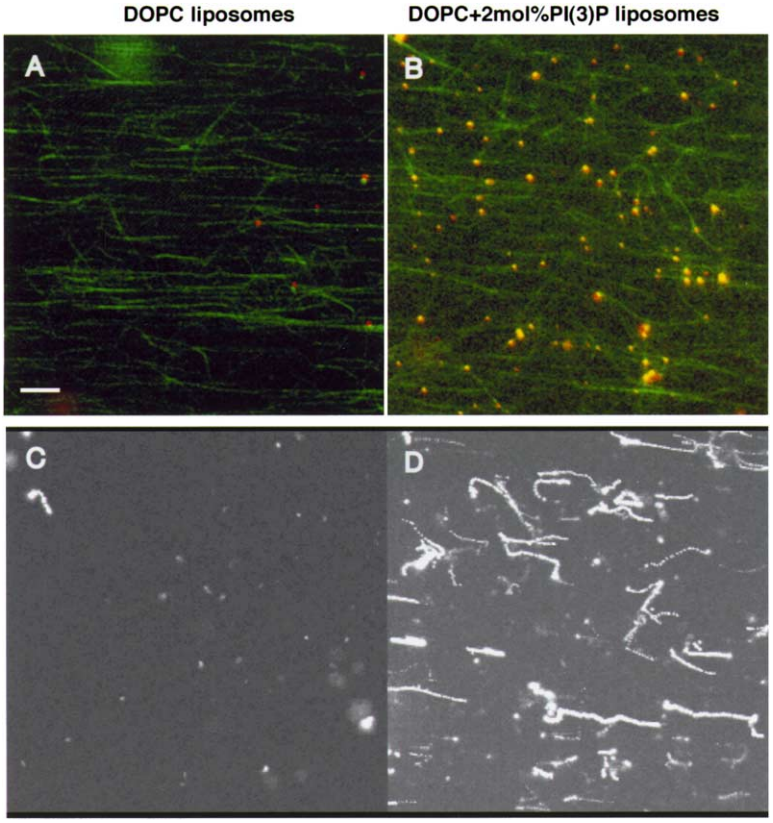

Figure 4. KIF16B Confers Motility to PI(3)P-Containing Liposomes In Vitro

The binding of KIF16B to and movement of liposomes in an in vitro motility assay depends on the presence of PI(3)P. Liposomes were composed of phosphatidylcholine and fluorescently labeled phosphatidylethanolamine, as a negative control (left panel), or the same mixture supplemented with 2 mol% of PI(3)P (right panel). Shown are still images of liposomes (red) and microtubules (green) in the top panel and collapsed video stacks displaying liposome movement in the bottom panel. PI(3)P-containing liposomes show motility along microtubules. Each collapsed movie represents 60 frames in a time resolution of one frame per 2 s. Scale bar, 5 μm.

Purified KIF16B Moves PI(3)P-Containing Liposomes along Microtubules In Vitro

Having established that the PX motif of KIF16B binds PI(3)P in vitro and localizes to membranes bearing this lipid in vivo, we next tested whether recombinant full-length KIF16B can be recruited onto PI(3)P-containing liposomes in a manner competent for transport. KIF16B was incubated with fluorescent liposomes with or without 2 mol% of PI(3)P. The suspension was applied to a chamber containing fluorescently labeled taxol-stabilized microtubules immobilized on the glass surface (Nielsen et al., 1999). True motility events, scored as movement of liposomes along the fluorescently labeled microtubule tracks, were differentiated from Brownian motion of immobile, microtubule bound liposomes. Whereas PI(3)P-free liposomes (Figures 4A and 4C) were unable to bind to microtubules (green) and diffused in the buffer in the presence of KIF16B, the PI(3)P-containing liposomes (Figures 4B and 4D) were recruited to and transported along microtubules, exhibiting continuous motion (displacement >3 μm) and velocity similar to microtubule gliding (Figure 2). These data provide further evidence that interaction of KIF16B with PI(3)P is sufficient to move liposomes in vitro.

KIF16B-Mediated Transport of Early Endosomes Depends on Rab5 and hVPS34 Activity

To test the hypothesis that KIF16B may participate in the Rab5- and PI(3)P-dependent early endosome motility (Nielsen et al., 1999), we first confirmed the presence of endogenous KIF16B on purified early endosomes. Endogenous KIF16B cofractionated with Rab5 and EEA1 (Figure 5A) on an early endosome-enriched fraction (Nielsen et al., 1999). Overexpression of KIF16B increased, whereas pretreatment of cells with Wortmannin reduced, the amount of EEA1 and KIF16B on the endosomal fraction (Figure 5A), consistent with PI(3)P being required for their membrane recruitment (Figures 3C and 3D).

The cofractionation with early endosomes prompted us to explore the activity of KIF16B in an assay that recapitulates the bidirectional movement of early endosomes in a cell-free system (Nielsen et al., 1999). In this assay, early endosomes, purified from HeLa cells fluorescently labeled by internalization of rhodamine-transferrin, are combined with cytosol, energy regenerating system, and buffered antifade mixture and perfused into a glass chamber coated by a uniform lawn of taxol-stabilized microtubules. Moving endosomes are analyzed by video microscopy. Since KIF16B moves toward the plus end of microtubules (Figure 2), we modified the experimental conditions to uncouple plus- from minus ended motility in the absence of cytosol (see Experimental Procedures). In this assay, the frequency of motility events, velocities, and lengths of movements of endosomes approximated the values from the cytosol-dependent assay. The motile endosomes exhibited track lengths and velocities similar to the PI(3)P-containing liposomes (Figures 5B and 5C). Addition of recombinant KIF16B stimulated the frequency of motility events (Figures 5E and 5F). Consistent with previous data (Nielsen et al., 1999), endosome

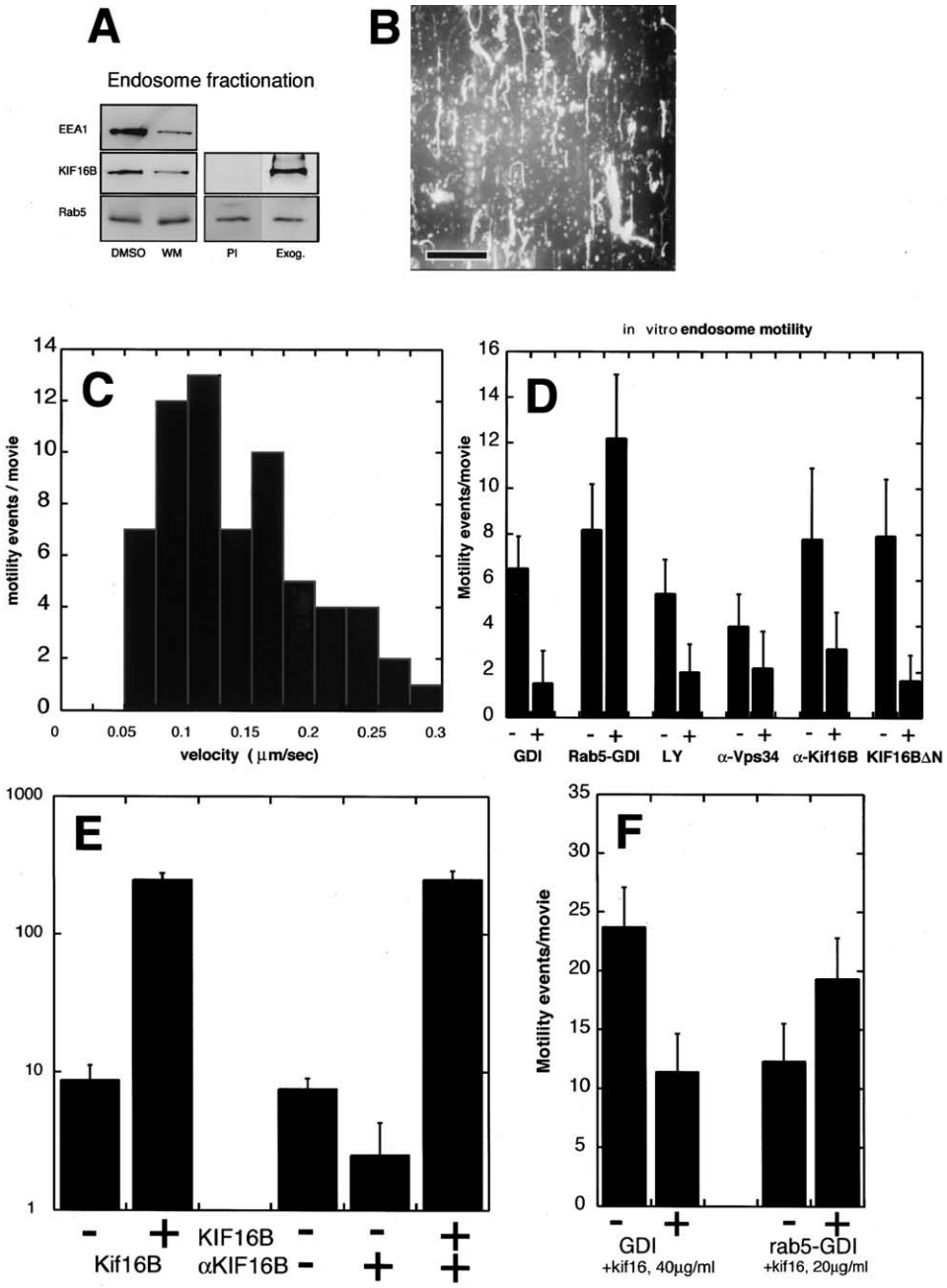

Figure 5. KIF16B Cofractionates with Early Endosomes and Modulates Plus End Motility of Early Endosomes in a Rab-5-Dependent Manner

(A) Early endosome-enriched fractions were analyzed by immunoblotting with EEA1, Rab5, and KIF16B antibodies. Endosomes purified from cells pretreated for 20 min with 100 nM Wortmannin (WM) show reduced amounts of EEA1 and KIF16B in comparison with endosomes from control cells (DMSO). Cells overexpressing exogenous KIF16B (Exog.) show an increased amount of KIF16B, while KIF16B preimmune serum shows no detectable signal on early endosomes.

(B) Rh-Transferin-labeled early endosomes move on microtubules in the presence of KIF16B. Shown are collapsed movie images from the in vitro motility assay (see Experimental Procedures). An image of a collapsed movie stack displays moving endosomes as continuous lines.

(C) The velocity distribution of moving endosomes in (B) shows motility events ranging from 0.05 to 0.3 μm/sec.

(D–F) The in vitro motility assay was carried out in the presence or absence (i.e., buffer or preimmune serum) of various reagents, and the recorded events per unit time were quantified (data are represented as mean ± SD). Inhibition of motility is seen in the presence of RabGDI, LY2344, truncated KIF16B protein, and antibodies against hVPS34 or KIF16B, while a stimulation of motility was observed upon addition of recombinant KIF16B or Rab5-GDI complex. The effect of the function blocking anti-KIF16B antibodies could be rescued by excess KIF16B protein (E). In the presence of exogenous KIF16B, early endosomes retained their responsiveness to the modulation of motility by Rab5 (F). Scale bar, 5 μm.

motility was Rab5 and PI(3)P dependent. First, extraction of Rab proteins from the endosome membrane with excess of RabGDI decreased, whereas addition of Rab5-GDI complex stimulated, the number of motility events (Figures 5D and 5F). Second, inhibition of PI(3)-kinase either by LY294002 or specific hVPS34 function-blocking antibodies (Nielsen et al., 1999) inhibited the motility of early endosomes (Figure 5D). Importantly, endosome motility along microtubules was not only stimulated by but also dependent on KIF16B activity. Movement was strongly inhibited by addition of either KIF16B-ΔN, a KIF16B deletion mutant protein lacking the catalytic domain, or affinity-purified anti-KIF16B antibodies. The antibody inhibition was specific, as it could be overcome by supplying recombinant KIF16B protein (Figure 5E). Furthermore, in the presence of exogenous KIF16B, the system maintained its sensitivity toward Rab-GDI and Rab5-GDI complex (compare Figure 5F with Figure 5D).

The finding that dominant-negative Rab5S34N displaces KIF16B from endosomes in vivo (Figure 4F), together with the dependence on Rab5 as well as hVPS34 activity for the motility in vitro, suggests that KIF16B is a motor protein that fulfils the biochemical properties previously established for the plus ended motility of early endosomes in vitro (Nielsen et al., 1999).

KIF16B Regulates the Steady-State Distribution of Early Endosomes

Having established a role of KIF16B in early endosome motility in vitro, we explored its function with respect to endosome distribution and transport in vivo. To this end, we compared the effects of full-length KIF16B-YFP overexpression in HeLa cells with silencing of the endogenous motor by RNA interference and the expression of two dominant-negative KIF16B mutants. The first one lacked the catalytic domain, retaining the stalk and PX domain unaltered (KIF16B-ΔN-YFP). Analogous truncation mutants have been reported to interfere with cargo localization (Noda et al., 2001). The second (KIF16B-S109A-YFP) had a point mutation in the nucleotide binding motif, thus impairing motor activity as shown for kinesin (Nakata and Hirokawa, 1995).

Opposite effects on the intracellular distribution of early endosomes were observed in these gain- and loss-of-function studies. While early endosomes strikingly relocalized to the cell periphery upon overexpression of KIF16B-YFP (Figure 6A), either of the two KIF16B mutants (Figures 6B and 6C) caused their clustering in the perinuclear region. A similar effect was produced by reducing KIF16B protein expression by ~90% using esiRNA (see Figure S1) (Figures 6E and 6F). Importantly, none of the various constructs resulted in any gross morphological alteration of the microtubule network, e.g., microtubule bundling or depolymerization (data not shown). These results suggest that, in regulating plus end motility, KIF16B governs the spatial distribution of early endosomes in vivo.

Ablation of KIF16B Expression Perturbs the Recycling Function of Early Endosomes

We next explored the role of KIF16B in the uptake of cargo into early endosomes, recycling to the surface, and delivery to late endocytic compartments. We first investigated whether the activity of KIF16B affects the transferrin (Tfn) cycle. Whereas overexpression of various KIF16B constructs did not impair uptake of Alexa568-labeled Tfn (Figure 6F, data not shown), ablation of KIF16B by RNAi accelerated its accumulation compared with mock-treated cells (Figures 6G and 6H). To quantify this effect, serum-starved HeLa cells were allowed to internalize biotinylated Tfn for various periods of time, washed, and lysed, and the intracellular fraction of Tfn was determined. Silencing of KIF16B indeed resulted in a faster rate of Tfn accumulation compared with control cells (Figure 6I). Since this effect could be due to a diminished recycling from early endosomes to the plasma membrane, we measured the kinetics of Tfn recycling, taking care not to chill cells to 4°C to avoid depolymerization of microtubules (Jin and Snider, 1993). Firstly, biotinylated Tfn was internalized into cells for 2 min. Under these conditions, endocytosed Tfn primarily reaches early endosomes but not perinuclear recycling endosomes. After a brief washing step to remove surface bound Tfn, cells were chased with 100-fold excess of unlabeled Tfn for different periods of time, and the amount of biotinylated Tfn retained in the cells was quantified. Silencing of KIF16B expression delayed Tfn recycling back to the plasma membrane in comparison to mock-treated cells (Figure 6H). Secondly, when the tracer was internalized for 1 hr to saturate perinuclear recycling endosomes, no inhibition of Tfn recycling was observed (compare Figures 6J and 6K), arguing that transport from recycling endosomes to the surface was not affected. These data suggest that, besides determining the distribution of early endosomes (Figure 5), KIF16B is also required for their efficient recycling of cargo to the cell surface.

KIF16B Overexpression or Ablation Alters EGF Trafficking In Vivo

Transport of cargo from early to late endosomes is microtubule dependent and requires the minus end motor dynein (Aniento et al., 1993). To investigate whether the accumulation of early endosomes underneath the cell cortex induced by overexpression of KIF16B impairs the sorting of cargo from early endosomes to the degradative pathway, we measured epidermal growth factor (EGF)-induced receptor internalization and degradation. HeLa cells expressing either wild-type or mutant KIF16B-S109A were stimulated with EGF for 30 min or 6 hr in the presence of cyclohexamide to prevent de novo synthesis of EGFR. Cells were subsequently processed for immunofluorescence staining with anti-EGFR antibodies and imaged by confocal microscopy, and signal intensities were quantified as described (Bache et al., 2003). In control cells, consistent with previous reports (Sorkin et al., 1991), EGFR was found in early and late endosomes during the first 30 min of EGF stimulation followed by almost complete degradation after 6 hr (Figure 7A). Overexpression of KIF16B but not KIF16B-S109A prevented EGF (data not shown) and EGFR from entering the degradative pathway. Strikingly, EGFR persisted in early endosomes at the cell cortex over 6 hr after internalization (Figure 7A). Under these conditions, the perinuclear localization of

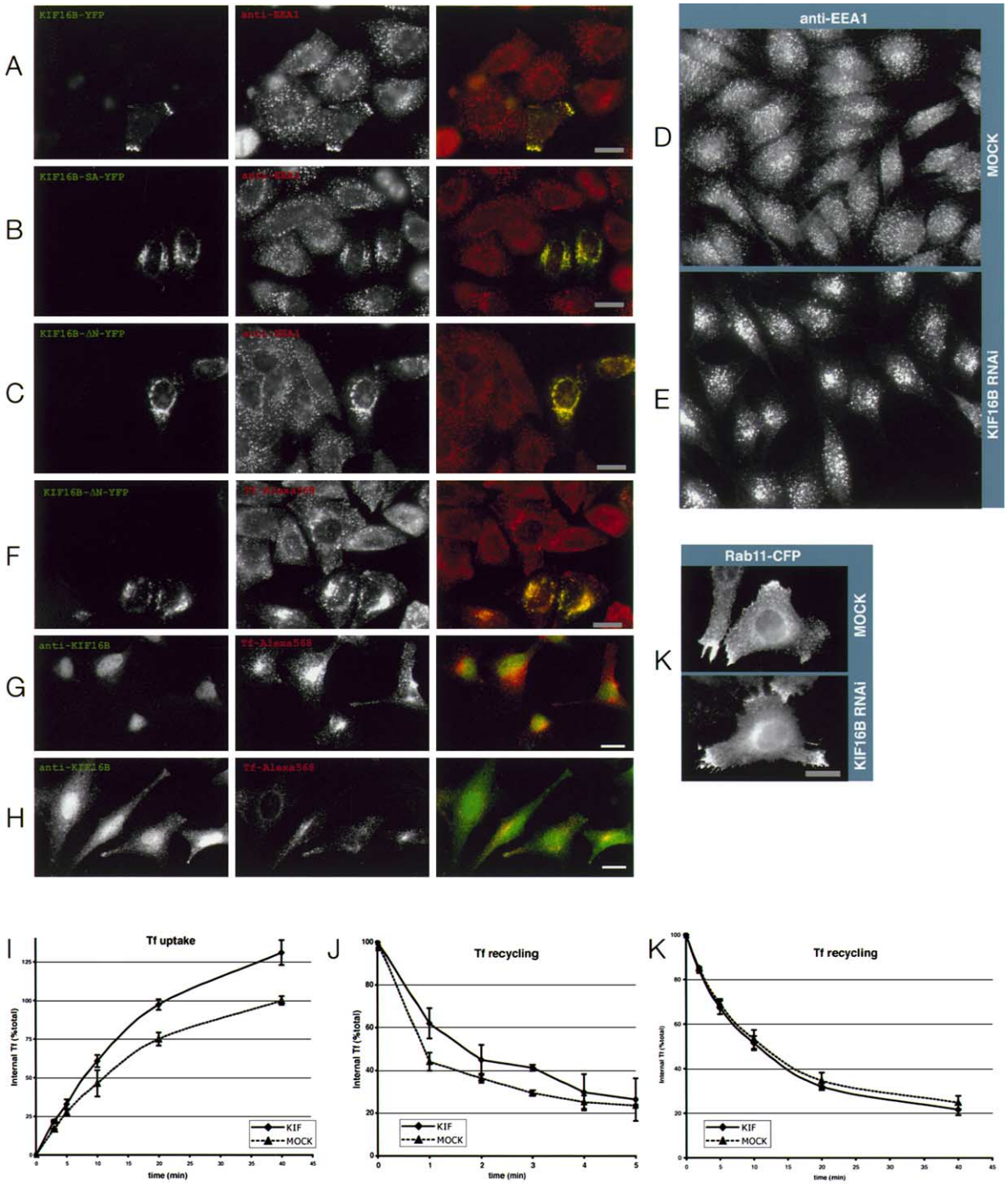

Figure 6. KIF16B Regulates the Steady-State Distribution of Early Endosomes and Is Required for Efficient Transferrin Recycling

HeLa cells were transfected with KIF16B-YFP ([A], green), KIF16B-ΔN-YFP ([B] and [F], green), or KIF16B-S109A-YFP (C). After transfection (24 hr), cells were immunostained with antibodies against EEA1 ([A]–[C], red) or pulsed with transferrin-Alexa568 for 30 min at 37°C followed by a 10 min chase to remove surface bound transferrin ([F], red). While EEA1 and transferrin-labeled endosomes translocate to the cell periphery upon overexpression of wild-type KIF16B (A), they cluster in the perinuclear region upon expression of the dominant negative constructs (B, C, and F). Also, knockdown of KIF16B results in centripetal translocation of early endosomes (D and E), while the morphology of Rab11-CFP-labeled recycling endosomes remains unaltered (K). (G, H, and I) Tfn uptake and recycling experiments. RNAi-treated HeLa cells were allowed to take up Alexa568-labeled Tfn for the indicated times and processed for fluorescence microscopy. Ablation of endogenous KIF16B (G) leads to an intracellular accumulation of Tfn (40 min) in comparison with mock-treated (H) cells. (I) Cells treated with unspecific (triangles) or KIF16B-specific esiRNA (squares) were allowed to take up biotinylated Tfn for the indicated times, washed, and lysed, and internalized Tfn was quantified. To examine if KIF16B function affects Tfn recycling from early endosomes (J) or from recycling endosomes (K), RNAi-treated cells were subjected to pulse chase experiments with biotinylated Tfn. Cells were loaded with Tfn for 2 min (J) or 1 hr (K), washed, and incubated at 37°C in medium containing 100-fold excess unlabeled Tfn. Internalized Tfn was quantified (see Experimental Procedures) and expressed as a percentage of total. Data from Tfn uptake and recycling assays are represented as mean ± SD. Scale bar, 20 μm.

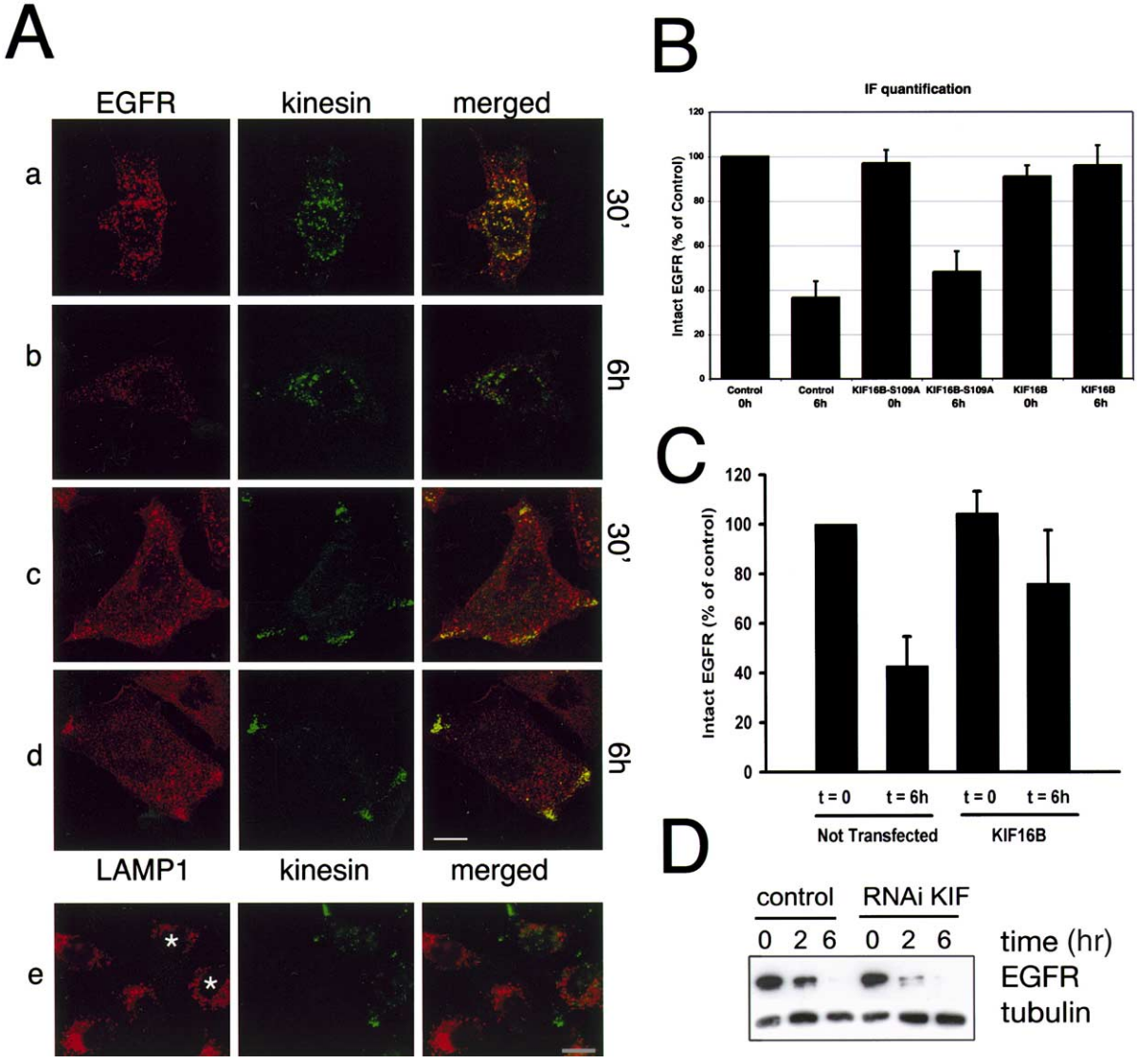

Figure 7. KIF16B Modulates the Degradation of Endocytosed EGFR

(A) HeLa cells were transfected with full-length KIF16B-YFP or dominant-negative KIF16-S109A-YFP constructs. Posttransfection (24 hr), the cells were induced with EGF (0.1 μM) in the presence of cycloheximide (10 μg/ml) for the indicated times and immunostained with antibodies to EGFR (Aa–Ad) or LAMP1 (Ae). Merge shows the superimposed confocal images of the kinesin (green) and EGFR or LAMP1 (red). Mock transfected cells (data not shown) as well as cells expressing KIF16-S109A-YFP almost completely degrade EGFR over the course of 6 hr (Aa and Ab). In contrast, overexpression of wild-type KIF16B-YFP inhibits EGFR degradation (Ac and Ad), while it does not affect localization of late endosomes stained with LAMP1 antibodies (Ae). The asterisks (*) mark the cell that overexpresses KIF16B.

(B) Quantification of EGFR signal (mean ± SEM) present in (A).

(C) Cells overexpressing KIF16B show significantly less degradation of EGFR. Cells were induced for the indicated times with EGF and immunoblotted for EGFR, and the blots were quantified. The amount of EGFR degraded is expressed as a percentage of total EGFR present before induction. The mean and SD from three independent experiments are shown.

(D) HeLa cells were induced for the indicated times with EGF and immunoblotted for EGFR and α-tubulin as a reference. Cells pretreated with RNAi specific for KIF16B show slightly accelerated degradation of EGFR as evident 2 hr after induction. Scale bar, 20 μm.

late endosomes, as visualized by LAMP1 staining, was unaffected (Figure 7A). That EGFR accumulated in early endosomes was indicated by the colocalization with Rab5, Tfn, EEA1, and PI(3)P but not the late endosome marker LAMP1 or lysotracker DND-99 (Figures 3 and 7 and Figure S1). All degradation kinetics of EGFR determined morphologically could also be confirmed biochemically (Figures 7B and 7C). Ablation of KIF16B by RNAi produced the opposite phenotype, i.e., accelerated the degradation of EGFR (Figure 7D). From these results, we conclude that KIF16B regulates the transport of cargo from early to late endosomes and, consequently, its degradation.

Discussion

The balance between plus and minus end-directed microtubule motors determines the intracellular local-

ization of early endosomes, recycling endosomes, late endosomes, and lysosomes. Here we report that KIF16B regulates the plus end motility of early endosomes and their intracellular distribution. With the findings that alterations of KIF16B function also affected the Tfn cycle and transport from early to late endosomes, we provide evidence for a role of this motor in regulating endosome location and the balance between receptor recycling and degradation.

KIF16B Is a Plus End Motor of Early Endosomes

KIF16B fulfils the functional properties expected for an early endosome kinesin. Motility studies indicated that the dynamic properties of recombinant KIF16B in vitro match some of the parameters measured for early endosome movement in vivo. First, KIF16B can transport membrane cargo over distances exceeding 3 μm, thus sustaining the long-range movement displayed by early endosomes in vivo (Gasman et al., 2003). The short-distance movements of early endosomes are due to the association with actin filaments promoted by the small GTPase RhoD (Gasman et al., 2003). Second, in HeLa cells, ~20% of Rab5-positive early endosomes move with velocities lower than 0.4 μm/sec, ~50% 0.4–0.8 μm/sec, and ~30% higher than 0.8 μm/s (Gasman et al., 2003). The velocities measured in vitro for KIF16B thus approximated the lower velocities of Rab5-labeled endosomes in vivo (velocity distribution around 0.35 μm/sec). Conventional KHC, which propels several types of organelles (Goldstein, 2001; Goodson et al., 1997; Hirokawa et al., 1998), displays ~2- to 3-fold higher velocities in vitro (Vale et al., 1985; von Massow et al., 1989). Early endosomes may well rely on multiple kinesins for propulsion, also depending on the cell type. For example, KIFC2, which was implicated in early endosomal motility, is likely restricted to neurons (Yang et al., 2001). However, besides its ubiquitous expression, a unique feature of KIF16B among KIFs is that it contains an important hallmark of early endosome targeting, the PX domain. This domain allows KIF16B to bind and move PI(3)P-containing liposomes and localize to early endosomes. Importantly, in vivo studies confirmed the idea that KIF16B is required for the proper intracellular distribution of early endosomes.

Next to the well-characterized Unc104/KIF1A, KIF16B represents the only other kinesin motor with the ability to directly interact with lipids. Since PX domains frequently require dimerization to bind PI(3)P (Lemmon, 2003), it is conceivable that the high coiled-coil potential of its stalk is sufficient for KIF16B to dimerize. This raises the question of whether the regulation of KIF16B motility follows a cooperative model, as proposed for Unc104 and Kif1A, for which clustering in lipid rafts leads to high density of motor monomers, thus facilitating dimerization and processive transport (Klopfenstein et al., 2002). Given its high coiled-coil propensity, KIF16B is in all likelihood a dimer like *D. discoideum* Unc104 and does not follow this cooperative transition upon recruitment to early endosomes.

Coupling of Membrane Fusion with Early Endosome Motility via Rab5 and PI(3)P

In displaying Rab5- and PI(3)P-containing cargo selectivity, a remarkable property of KIF16B is that it is subjected to the same regulatory principles governing the membrane tethering and fusion machinery (Zerial and McBride, 2001). Even though Rab5 and KIF16B do not appear to interact directly, Rab5 can modulate the generation of PI(3)P in its vicinity via its direct interaction with hVPS34/p150 (Christoforidis et al., 1999) (Shin, personal communication), thus allowing for the binding of the PX domain of KIF16B to the endosomal membrane. This mechanism reiterates the role of Rab5 in creating a specialized membrane domain in which the activities of different effectors can be kinetically controlled by the GTPase cycle and coordinated through spatial segregation within restricted subcompartments of the early endosome (Zerial and McBride, 2001).

Our study strengthens the emerging paradigm that Rab GTPases, besides functioning in membrane fusion, also orchestrate organelle movement. Rab11 and Rab27 regulate the membrane recruitment of myosin motors onto recycling endosomes and melanosomes (Hales et al., 2002; Wu et al., 2002). Rabkinesin-6 was proposed to be an effector of Rab6 regulating the movement of Golgi membranes (Echard et al., 1998), although recent studies argue, rather, for a function in cytokinesis (Hill et al., 2000). Finally, the Rab7 effector RILP was shown to indirectly regulate the recruitment of the dynein-dynactin complex to late endosomes (Jordens et al., 2001).

In the case of early endosomes, Rab5 and PI(3)P appear to regulate both the plus- and minus end motility of early endosomes (Nielsen et al., 1999), raising the question of how bidirectional movement is regulated. For example, the bidirectional movement of melanosomes is coordinated by dynactin, which binds both dynein and the plus end motor kinesin II (KIF3) (Deacon et al., 2003; Valetti et al., 1999). In the absence of cytosol, isolated early endosomes exhibit only plus end motility in vitro, suggesting that minus end-directed motors must either be lost or inactivated during the fractionation procedure. However, rather than the direction of movement being determined by stochastic motor recruitment or competition between motors of opposite polarity, precise regulatory mechanisms are required to switch them on and off (Reilein et al., 2001). A possible regulatory mechanism for the activity of KIF16B could be phosphorylation, given the presence of a phosphothreonine/serine binding FHA domain (Durocher and Jackson, 2002).

The Role of KIF16B in Endosome Motility, Cargo Transport, and Signal Transduction

Our data suggest that microtubule-dependent motility plays a role in the regulation of endocytic transport at earlier stages than previously assumed. Microtubule-dependent motility facilitates trafficking from early to late endosomes but is not required for the recycling of ligand/receptor complexes from early endosomes to the surface (Apodaca, 2001), a process that rather depends on actin (Apodaca, 2001). Our data suggest that plus end motility along microtubules may facilitate the targeting of recycling carriers from early endosomes to the plasma membrane. This may be a prerequisite to switch from microtubule- to actin-based transport to allow efficient cargo exocytosis. Proximity of early endosomes to the cell cortex may also favor fast over slow

recycling via perinuclear recycling endosomes (Maxfield and McGraw, 2004), as also observed for Rabenosyn-5 (de Renzis et al., 2002). Interestingly, inhibitors of PI(3)-kinase cause a significant retention of transferrin in early endosomes (van Dam et al., 2002). Such inhibition could be explained, at least in part, by the release of KIF16B from the early endosome membrane (Figure 3).

Transport along the degradative pathway, either mediated by endosomal carrier vesicles (ECVs) that bud from early and fuse with late endosomes or occurring by a maturation process (Gruenberg and Maxfield, 1995), has been shown to exclusively depend on dynein (Aniento et al., 1993). Our findings that KIF16B modulates EGFR degradation suggest that the activity of KIF16B balances that of dynein in regulating the transport of cargo from early to late endosomes. We have observed that transition from early to late endosomes occurs by conversion of Rab5-positive into Rab7-positive structures, a process occurring near the center of the cell (Rink, personal communication). Based on the effects of KIF16B, we suggest that the spatial distribution of early endosomes is critical to their ability to either generate ECVs or convert into late endosomes. Consistently, the peripheral endosomes induced by KIF16B overexpression harbored early but failed to acquire late endosome markers. We propose that early endosomes can acquire cargo and recycle it to the cell surface as long as the Rab5 and PI(3)P-dependent recruitment of KIF16B keeps them near the periphery. Once the activity of dynein prevails over that of KIF16B, the endosomes predominantly reside in the center of the cell where they become committed to switch to the degradative pathway. Interestingly, when late endosomes were relocated to the cortex of the cell by dynamitin overexpression, transport from early to late endosomes was inhibited despite the close proximity of these organelles to each other (Valetti et al., 1999), further supporting the idea that intracellular localization governs the transport activity of these organelles.

Our results on the effect of KIF16B on EGF degradation have important implications for signal transduction. Prior to degradation, internalized receptors continue signaling by activating cytoplasmic target molecules (Miaczynska et al., 2004). Since receptor downregulation results in signal desensitization over time, the trafficking role of KIF16B may also impact on the signaling response. Remarkably, KLP98A, the *Drosophila* ortholog of KIF16B, has previously been linked to *wingless* (*wg*) signaling (Dalby et al., 1996), opening the interesting avenue of exploring the role of KIF16B during development. It will also be interesting to explore the role of KIF16B in endocytic and transcytotic trafficking in polarized cells. Addressing these questions will improve our understanding of the physiological role of cytoskeleton-mediated endocytic transport at the cellular and multicellular levels.

Experimental Procedures

Antibodies and Other Reagents

Anti-tubulin antibody (1:250) was from Sigma-Aldrich; polyclonal anti-EEA1 (1:500) (Christoforidis et al., 1999) and anti-LAMP1 (1:500) from PharMingen; and anti-vps34 (Nielsen et al., 1999), sheep anti-EGF receptor (Fitzgerald; 1:1000) and rhodamine-conjugated transferrin from Molecular Probes. LY294002 and Wortmannin were obtained from Calbiochem-Novabiochem GmbH. Cell culture reagents were from Sigma-Aldrich and Invitrogen. Other chemicals were from Sigma, unless specified.

Cell Transfection, Immunofluorescence Microscopy, and Time-Lapse Fluorescence Video Microscopy

HeLa cell transfection was carried out using Effectene (Quiagene)/DNA complex. Oligofectamine (Invitrogen) was utilized for esiRNA transfection. After 24 hr (DNA) or 72 hr (RNA), cells were used for analysis. For videomicroscopy, cells transiently expressing GFP-Rab5 or YFP-KIF16B grown on glass coverslips were transferred to custom-built aluminium microscope slide chambers just before observation. Time-lapse imaging was performed at 37°C and analyzed using customized software (Gasman et al., 2003).

cDNA Cloning, Sequence Analysis, Northern Blot, and RNA Interference

KIF16B was cloned from HeLa total mRNA using ATGAGCGATGG CATCGGTC and CTACCCCGTCCCGTGGCTG primers. The full-length construct was subcloned into pEYFP-N1 (CLONTECH, Palo Alto, CA) by ET recombination. For the headless KIF16B constructs, carboxyl terminal sequences of human KIF16B were amplified from full-length KIF16B cDNA using PCR and subsequently cloned into pEYFP-N1 and pGEX-6P-1 to obtain KIF16B-ΔN (aa 396–1318) and KIF16B-ΔN2 (aa 219–1318) fusion constructs. The KIF16B-S109A construct was created by site-directed mutagenesis using the QuikChange Site-Directed Mutagenesis Kit (Stratagene). The GST-KIF16B-PX construct was made by subcloning the C terminus (aa 1169–1318) of KIF16B into EcoRI/SalI sites of pGEX-6P-1 following standard methods. All constructs were verified by DNA sequencing. Coils prediction of the protein sequences was run with weighing option window size of 28 for KHC, DdKIF1A, and HsKIF16B and 21 for HsKIF1A. A human tissue Northern blot purchased from BD Biosciences was probed for KIF16B mRNA (CTGGATTTGCGCCCAAAGAGCG, CAGAGAGAGGCGCTGGAGCGG) using the Dig Northern kit (Roche). KIF16B-specific esiRNA was prepared as described (Yang et al., 2002) using GTAATACGACT CACTATAGGCAGGAGATCCTAGAG and GTAATACGACTCACTATAG GGCCCAGGGTGGAGTG primers.

Polyclonal Antibody Generation, Affinity Purification, Subcellular Fractionation, and Immunoblotting

Truncated KIF16B-ΔN (aa 396–1318) protein was expressed and purified as GST fusion protein in *E. coli*, cleaved from GST, and injected into rabbits (Elevage Scientifique des Dombes, France). The antiserum was affinity purified using the antigen protein immobilized on Sulfolink beads (Pierce). An early endosome-enriched fraction was purified from HeLa cells mock treated or treated with 100 nM Wortmannin for 30 min in 37°C as described (Nielsen et al., 1999). The endosomes were subsequently analyzed using SDS-PAGE chromatography and immunoblotting or used for in vitro motility studies.

In Vitro Motility, Microtubules Gliding, and Liposome Assays

The in vitro motility assay was essentially carried out as described (Nielsen et al., 1999) with the following modification: KHMG (110 mM KCl, 50 mM HEPES-KOH [pH 7.4], 2 mM $MgCl_2$, 10% glycerol) was used as assay buffer. For preparation of the antifade solution, BRB80 buffer was substituted with KHMG and the solution was supplemented with 10% serum. The energy mix consisted of 75 mM creatine phosphate, 10 mM ATP, 10 mM GTP, and 20 mM $MgCl_2$ in BRB80. Fluorescently labeled, taxol-stabilized microtubules were perfused in a microscopy chamber to bind to the coverslip (Nielsen et al., 1999). Next, 10 μl of 10% nonspecific rabbit serum in antifade solution was perfused in the chamber followed by 10 μl of the assay mixture (2 μl fluorescently labeled endosomes [5 mg/ml], 1 μl energy mix, 6 μl antifade solution, and 1 μl saturated haemoglobin solution in KHMG) and incubated for 5 min at RT. At least three movies per sample were recorded (60 frames, 2 s intervals) and analyzed as described (Nielsen et al., 1999). When endosomal movement was analyzed using centrosome-grown microtubules, all 25 recorded motility events observed were plus end

directed. Liposomes were prepared as described (Klopfenstein et al., 2002) using DOPC, 2 mol% PI(3)P (Echelon Research Laboratories) and 0.5 mol% TRITC-DHPE (Molecular Probes) diluted 1:100 in KHEM. To determine the directionality of the motor in the microtubule-gliding assay, HIS-tagged full-length KIF16B was purified using a baculovirus system, and 10 μl of recombinant KIF16B (0.4 mg/ml) was left on a coverslip for 5 min and washed with KHMG, and 3 μl of the polarity-marked microtubules were added in BRB80 buffer containing 1 mM ATP as described (Nielsen et al., 1999). To quantify the velocity of the motor-induced microtubule gliding, taxol-stabilized instead of polarity-marked microtubules were used.

Transferrin Uptake, Recycling, and EGFR Degradation

For the transferrin internalization assay, HeLa cells were transfected with KIF16B-EYFP expression vector or esiRNA specific for KIF16B or a pBluescript vector sequence (mock). At 16 hr (DNA) or 74 hr (esiRNA) posttransfection, cells were starved for 4 hr in CO2-independent DMEM medium containing 0.2%BSA and then incubated with Alexa568-labeled Tfn (Sigma-Aldrich) at 0.5 mg/ml for the indicated times. For biochemical uptake analysis, starved cells were allowed to internalize biotinylated Tfn (10 μg/ml) for the times indicated. Cells were placed on ice, washed, and lysed, and the total cell extract was incubated with affinity-purified, ruthenium-labeled, sheep-anti-human Tfn antibodies (SAPU, Scotland) and subsequently analyzed using an ECL-Analyzer System from IGEN Inc. (Rockville, MD). The amount of internalized Tfn was standardized with respect to total protein concentration of the lysate and expressed as percent of the amount of internalized Tfn in control cells at t = 40 min (n = 4; mean ± SD from two independent experiments). The Tfn recycling assay was carried out as described (de Renzis et al., 2002), except that cells were rapidly washed once at 37°C with CO2-independent DMEM with 100 μg/ml human holo-Tfn (n = 4; mean ± SD from two independent experiments). EGF-stimulated EGFR uptake and degradation were either studied by confocal microscopy and image processing (Bache et al., 2003) or measured biochemically. For EGFR degradation (5×10^5, 5 cm dishes), HeLa cells were transfected for 24 hr with 400 ng of the indicated plasmid, using Effectene (R). The cells were then incubated with or without 100 ng/ml EGF for 30 min, washed, and chased for 6 hr in normal growth medium containing 10 μg/ml cycloheximide. Cell extracts were then analyzed by SDS-PAGE and Western blotting with anti-EGFR antibodies.

Supplemental Data

Supplemental Data include one figure and six movies and can be found with this article online at http://www.cell.com/cgi/content/full/121/3/437/DC1/.

Acknowledgments

We are indebted to R. Kittler for his advice on esiRNAi technology and Y. Kalaidzidis for the in vivo velocity quantitation. We would like to thank Drs. J. Howard, K. Simons, M. Miaczynska, and S. Eaton for valuable comments on the paper and discussions. This work was supported by grants from the HFSP (RG-0260/1999-M), the European Union (HPRN-CT-2000-00081), and the Max Planck Society.

Received: May 14, 2004
Revised: September 27, 2004
Accepted: February 16, 2005
Published: May 5, 2005

References

Allan, V. (2000). Dynactin. Curr. Biol. *10*, R432.

Aniento, F., Emans, N., Griffiths, G., and Gruenberg, J. (1993). Cytoplasmic dynein-dependent vesicular transport from early to late endosomes. J. Cell Biol. *123*, 1373–1387.

Apodaca, G. (2001). Endocytic traffic in polarized epithelial cells: role of the actin and microtubule cytoskeleton. Traffic *2*, 149–159.

Aschenbrenner, L., Naccache, S.N., and Hasson, T. (2004). Uncoated endocytic vesicles require the unconventional myosin, Myo6, for rapid transport through actin barriers. Mol. Biol. Cell *15*, 2253–2263.

Bache, K.G., Raiborg, C., Mehlum, A., and Stenmark, H. (2003). STAM and Hrs are subunits of a multivalent ubiquitin-binding complex on early endosomes. J. Biol. Chem. *278*, 12513–12521.

Burkhardt, J.K., Echeverri, C.J., Nilsson, T., and Vallee, R.B. (1997). Overexpression of the dynamitin (p50) subunit of the dynactin complex disrupts dynein-dependent maintenance of membrane organelle distribution. J. Cell Biol. *139*, 469–484.

Case, R.B., Pierce, D.W., Hom-Booher, N., Hart, C.L., and Vale, R.D. (1997). The directional preference of kinesin motors is specified by an element outside of the motor catalytic domain. Cell *90*, 959–966.

Christoforidis, S., Miaczynska, M., Ashman, K., Wilm, M., Zhao, L., Yip, S.C., Waterfield, M.D., Backer, J.M., and Zerial, M. (1999). Phosphatidylinositol-3-OH kinases are Rab5 effectors. Nat. Cell Biol. *1*, 249–252.

Dalby, B., Pesavento, P.A., and Goldstein, L.S.B. (1996). A novel kinesin like motor involved in Wingless (WNT) signaling in *Drosophila*. Mol. Biol. Cell Suppl. *7*, 487a.

Deacon, S.W., Serpinskaya, A.S., Vaughan, P.S., Lopez Fanarraga, M., Vernos, I., Vaughan, K.T., and Gelfand, V.I. (2003). Dynactin is required for bidirectional organelle transport. J. Cell Biol. *160*, 297–301.

de Renzis, S., Sonnichsen, B., and Zerial, M. (2002). Divalent Rab effectors regulate the sub-compartmental organization and sorting of early endosomes. Nat. Cell Biol. *4*, 124–133.

Durocher, D., and Jackson, S.P. (2002). The FHA domain. FEBS Lett. *513*, 58–66.

Echard, A., Jollivet, F., Martinez, O., Lacapere, J.J., Rousselet, A., Janoueix-Lerosey, I., and Goud, B. (1998). Interaction of a Golgi-associated kinesin-like protein with Rab6. Science *279*, 580–585.

Gasman, S., Kalaidzidis, Y., and Zerial, M. (2003). RhoD regulates endosome dynamics through Diaphanous-related Formin and Src tyrosine kinase. Nat. Cell Biol. *5*, 195–204.

Gillooly, D.J., Morrow, I.C., Lindsay, M., Gould, R., Bryant, N.J., Gaullier, J.M., Parton, R.G., and Stenmark, H. (2000). Localization of phosphatidylinositol 3-phosphate in yeast and mammalian cells. EMBO J. *19*, 4577–4588.

Goldstein, L.S. (2001). Molecular motors: from one motor many tails to one motor many tales. Trends Cell Biol. *11*, 477–482.

Goodson, H.V., Valetti, C., and Kreis, T.E. (1997). Motors and membrane traffic. Curr. Opin. Cell Biol. *9*, 18–28.

Gruenberg, J., and Maxfield, F.R. (1995). Membrane transport in the endocytic pathway. Curr. Opin. Cell Biol. *7*, 552–563.

Hales, C.M., Vaerman, J.P., and Goldenring, J.R. (2002). Rab11 family interacting protein 2 associates with Myosin Vb and regulates plasma membrane recycling. J. Biol. Chem. *277*, 50415–50421.

Hill, E., Clarke, M., and Barr, F.A. (2000). The Rab6-binding kinesin, Rab6-KIFL, is required for cytokinesis. EMBO J. *19*, 5711–5719.

Hirokawa, N., Noda, Y., and Okada, Y. (1998). Kinesin and dynein superfamily proteins in organelle transport and cell division. Curr. Opin. Cell Biol. *10*, 60–73.

Howard, J., Hudspeth, A.J., and Vale, R.D. (1989). Movement of microtubules by single kinesin molecules. Nature *342*, 154–158.

Hyman, A.A. (1991). Preparation of marked microtubules for the assay of the polarity of microtubule-based motors by fluorescence. J. Cell Sci. Suppl. *14*, 125–127.

Jin, M., and Snider, M.D. (1993). Role of microtubules in transferrin receptor transport from the cell surface to endosomes and the Golgi complex. J. Biol. Chem. *268*, 18390–18397.

Jordens, I., Fernandez-Borja, M., Marsman, M., Dusseljee, S., Janssen, L., Calafat, J., Janssen, H., Wubbolts, R., and Neefjes, J. (2001). The Rab7 effector protein RILP controls lysosomal transport

by inducing the recruitment of dynein-dynactin motors. Curr. Biol. *11*, 1680–1685.

Klopfenstein, D.R., Tomishige, M., Stuurman, N., and Vale, R.D. (2002). Role of phosphatidylinositol(4,5)bisphosphate organization in membrane transport by the Unc104 kinesin motor. Cell *109*, 347–358.

Lawrence, C.J., Dawe, R.K., Christie, K.R., Cleveland, D.W., Dawson, S.C., Endow, S.A., Goldstein, L.S., Goodson, H.V., Hirokawa, N., Howard, J., et al. (2004). A standardized kinesin nomenclature. J. Cell Biol. *167*, 19–22.

Lemmon, M.A. (2003). Phosphoinositide recognition domains. Traffic *4*, 201–213.

Lin, S.X., Gundersen, G.G., and Maxfield, F.R. (2002). Export from pericentriolar endocytic recycling compartment to cell surface depends on stable, detyrosinated (glu) microtubules and kinesin. Mol. Biol. Cell *13*, 96–109.

Lupas, A., Van Dyke, M., and Stock, J. (1991). Predicting coiled coils from protein sequences. Science *252*, 1162–1164.

Maxfield, F.R., and McGraw, T.E. (2004). Endocytic recycling. Nat. Rev. Mol. Cell Biol. *5*, 121–132.

Mellman, I. (1996). Endocytosis and molecular sorting. Annu. Rev. Cell Dev. Biol. *12*, 575–625.

Miaczynska, M., Pelkmans, L., and Zerial, M. (2004). Not just a sink: endosomes in control of signal transduction. Curr. Opin. Cell Biol. *16*, 400–406.

Miki, H., Setou, M., and Hirokawa, N. (2003). Kinesin superfamily proteins (KIFs) in the mouse transcriptome. Genome Res. *13*, 1455–1465.

Nakata, T., and Hirokawa, N. (1995). Point mutation of adenosine triphosphate-binding motif generated rigor kinesin that selectively blocks anterograde lysosome membrane transport. J. Cell Biol. *131*, 1039–1053.

Nielsen, E., Severin, F., Backer, J.M., Hyman, A.A., and Zerial, M. (1999). Rab5 regulates motility of early endosomes on microtubules. Nat. Cell Biol. *1*, 376–382.

Noda, Y., Okada, Y., Saito, N., Setou, M., Xu, Y., Zhang, Z., and Hirokawa, N. (2001). KIFC3, a microtubule minus end-directed motor for the apical transport of annexin XIIIb-associated Triton-insoluble membranes. J. Cell Biol. *155*, 77–88.

Okada, Y., Yamazaki, H., Sekine-Aizawa, Y., and Hirokawa, N. (1995). The neuron-specific kinesin superfamily protein KIF1A is a unique monomeric motor for anterograde axonal transport of synaptic vesicle precursors. Cell *81*, 769–780.

Pollock, N., de Hostos, E.L., Turck, C.W., and Vale, R.D. (1999). Reconstitution of membrane transport powered by a novel dimeric kinesin motor of the Unc104/KIF1A family purified from Dictyostelium. J. Cell Biol. *147*, 493–506.

Reilein, A.R., Rogers, S.L., Tuma, M.C., and Gelfand, V.I. (2001). Regulation of molecular motor proteins. Int. Rev. Cytol. *204*, 179–238.

Shmueli, O., Horn-Saban, S., Chalifa-Caspi, V., Shmoish, M., Ophir, R., Benjamin-Rodrig, H., Safran, M., Domany, E., and Lancet, D. (2003). GeneNote: whole genome expression profiles in normal human tissues. C. R. Biol. *326*, 1067–1072.

Sorkin, A., Krolenko, S., Kudrjavtceva, N., Lazebnik, J., Teslenko, L., Soderquist, A.M., and Nikolsky, N. (1991). Recycling of epidermal growth factor-receptor complexes in A431 cells: identification of dual pathways. J. Cell Biol. *112*, 55–63.

Vale, R.D. (2003). The molecular motor toolbox for intracellular transport. Cell *112*, 467–480.

Vale, R.D., Reese, T.S., and Sheetz, M.P. (1985). Identification of a novel force-generating protein, kinesin, involved in microtubule-based motility. Cell *42*, 39–50.

Valetti, C., Wetzel, D.M., Schrader, M., Hasbani, M.J., Gill, S.R., Kreis, T.E., and Schroer, T.A. (1999). Role of dynactin in endocytic traffic: effects of dynamitin overexpression and colocalization with CLIP-170. Mol. Biol. Cell *10*, 4107–4120.

van Dam, E.M., Ten Broeke, T., Jansen, K., Spijkers, P., and Stoorvogel, W. (2002). Endocytosed transferrin receptors recycle via distinct dynamin and phosphatidylinositol 3-kinase-dependent pathways. J. Biol. Chem. *277*, 48876–48883.

von Massow, A., Mandelkow, E.M., and Mandelkow, E. (1989). Interaction between kinesin, microtubules, and microtubule-associated protein 2. Cell Motil. Cytoskeleton *14*, 562–571.

Wu, X.S., Rao, K., Zhang, H., Wang, F., Sellers, J.R., Matesic, L.E., Copeland, N.G., Jenkins, N.A., and Hammer, J.A., 3rd. (2002). Identification of an organelle receptor for myosin-Va. Nat. Cell Biol. *4*, 271–278.

Yang, Z., Roberts, E.A., and Goldstein, L.S. (2001). Functional analysis of mouse C-terminal kinesin motor KifC2. Mol. Cell. Biol. *21*, 2463–2466.

Yang, D., Buchholz, F., Huang, Z., Goga, A., Chen, C.Y., Brodsky, F.M., and Bishop, J.M. (2002). Short RNA duplexes produced by hydrolysis with *Escherichia coli* RNase III mediate effective RNA interference in mammalian cells. Proc. Natl. Acad. Sci. USA *99*, 9942–9947.

Zerial, M., and McBride, H. (2001). Rab proteins as membrane organizers. Nat. Rev. Mol. Cell Biol. *2*, 107–117.

Zhou, H.M., Brust-Mascher, I., and Scholey, J.M. (2001). Direct visualization of the movement of the monomeric axonal transport motor UNC-104 along neuronal processes in living *Caenorhabditis elegans*. J. Neurosci. *21*, 3749–3755.